Deblending using hybrid Radon transform

Amr Ibrahim, Kai Zhuang, and Daniel Trad

ABSTRACT

In this report, we add a hybrid Radon transform to the inversion-based deblending method. Deblending methods that use sparsity constraint relies on the similarity between the primary signal and the transform basis. This similarity results in the focusing of the coherent primary signal while simultaneously attenuating the incoherent blending noise. However, seismic data contains mixtures of signals with different travel time trajectories. Therefore, using hyperbolic functions to model seismic data that contains non-hyperbolic events will reduce sparsity (signal focusing) and thereby reduce the efficiency of the deblending algorithm. To overcome this issue, we expand the transform basis to account for more types of signals contained in the seismic data. In this report, we a hybrid of linear and hyperbolic Radon basis functions to match the moveout patterns of reflections and direct arrivals. Synthetic data examples show that this transform can efficiently deblend seismic reflections and direct arrivals.

INTRODUCTION

Blended seismic acquisition is becoming a more appropriate technique to increase seismic illumination of the subsurface without increasing survey cost (Berkhout et al., 2008). We can group the deblending methods in literature into three main categories. The first category uses a conventional seismic processing sequence for blended data without separation. These passive deblending methods utilize the power of stacking in the traditional processing sequence to suppress source interferences. The second category of deblending methods, treat interferences as noise, and use a denoising algorithm to remove them (Trad et al., 2012; Ibrahim and Sacchi, 2014). The third category of deblending methods, interpret interferences as a signal and cast the deblending problem as an inversion problem. In either denoising-based and inversion-based deblending methods, the choice of the sparse transform can be critical to the success of deblending algorithms. Therefore, designing transforms that can represent seismic data by a few (sparse) coefficients is an important research topic. Inversion algorithms that are constrained by sparsity have proved to be a powerful tool in seismic data processing, especially for denoising and interpolation (Ibrahim et al., 2018) applications. The ability of a transform to represent the data as a sparse summation of weighted basis functions is directly related to the similarity between the transform basis functions and the main components of the data. For this reason, it is desirable to tailor the transform basis functions to resemble the main components of seismic data as close as possible.

In general, we can divide sparse transforms into two broad categories, model-driven transforms, and data-driven transforms (Zhu et al., 2015). Model-driven transforms use a formulated mathematical model of the data, which leads to pre-defined basis functions (dictionary). For example, the mathematical model for the Fourier transform assumes that the data are composed of sinusoidal basis functions. Several model-driven transforms have been commonly used for sparse inversion of seismic data such as Fourier (Sacchi et al.,

1998), Radon (Thorson and Claerbout, 1985), wavelet (Sinha et al., 2005), curvelet (Herrmann and Hennenfent, 2008), seislet (Fomel and Liu, 2010), contourlet (Shan et al., 2009) and focal transforms (Berkhout and Verschuur, 2006). On the other hand, data-driven transforms learns the basis functions from the data and do not have pre-defined basis functions. Data-driven transforms learn its basis functions from the data which tailor the transform basis functions for sparse representation. Therefore, data-driven transforms can be more adaptable to changes in the structure of observed seismic data than the model-based transforms. Recently, data-driven transforms have been used in seismic data processing for denoising (Chen and Sacchi, 2015), interpolation (Yu et al., 2015), and source separation (Cheng and Sacchi, 2015). However, data-driven transforms have a high computational cost and require the storage of the transform basis functions learned from the training data sets used in dictionary learning. Therefore, it is desirable to design computationally efficient model-based transforms with pre-defined basis functions that match the main components of seismic data (Ibrahim, 2015; Ibrahim et al., 2018).

THEORY

Radon transforms

To derive the general formulation for Radon operators, let us assume that $d(t,x)$ denote the two dimensional seismic data and $m(\tau,\xi)$ denote the Radon model (Sacchi and Ulrych, 1995). We first define the forward Radon operator, $\mathscr{L}$, and its adjoint operator $\mathscr{L}^\dagger$ as follow

$$d(t,x) = \mathscr{L}\, m(\tau,\xi) = \int_{-\infty}^{\infty} m(\tau = \phi\,(t,x,\xi),\xi)\, d\xi, \tag{1}$$

$$\widetilde{m}(\tau,\xi) = \mathscr{L}^\dagger\, d(t,x) = \int_{-\infty}^{\infty} d(t = \widetilde{\phi}\,(\tau,x,\xi),x)\, dx, \tag{2}$$

where $\widetilde{m}(\tau,\xi)$ is the Radon model estimated by the adjoint operator. The parameter ξ is the Radon parameter (or parameters) that define the Radon operator integration path by the function $\phi(\tau,x,\xi)$. Radon transform operators are adaptable, and they can use many different geometrical curves as their integration path. Popular variants of the Radon transform operators are linear (LRT), parabolic (PRT) and hyperbolic Radon (HRT) operators. Table 1 lists the different forward and adjoint Radon operators used in seismic data processing. In table 1, p represents the ray parameter and v represents velocity.

Table 1. Common Radon transforms.

Operator	$\widetilde{\phi}\,(\tau,x,\xi)$	$\phi\,(t,x,\xi)$
LRT (slant stack)	$t = \tau + p\,x$	$\tau = t - p\,x$
PRT	$t = \tau + q\,x^2$	$\tau = t - q\,x^2$
HRT (velocity stack)	$t = \sqrt{\tau^2 + \frac{x^2}{v^2}}$	$\tau = \sqrt{t^2 - \frac{x^2}{v^2}}$

HYBRID RADON TRANSFORM

The conventional hyperbolic Radon operator assumes that the minimum two-way travel time for seismic reflections is located at zero offset and the data can be modelled as a superposition of reflection hyperbolas as,

$$d(t,h) = \int_{v_{min}}^{v_{max}} m(\tau = \sqrt{t^2 - \frac{h^2}{v^2}}, v)\, dv\,. \tag{3}$$

However, this is not generally true, especially in common shot or common receiver gathers, Therefore, the HRT operator should be expanded to include scanning for travel time apexes

$$d(t,h) = \int_{a_{min}}^{a_{max}} \int_{v_{min}}^{v_{max}} m(\tau = \sqrt{t^2 - \frac{(h-a)^2}{v^2}}, v)\, dv\, da\,, \tag{4}$$

and the adjoint operator will be

$$m(\tau,v,a) = \int_{h_{min}}^{h_{max}} d(t = \sqrt{\tau^2 + \frac{(h-a)^2}{v^2}}, h)\, dh\,, \tag{5}$$

where a is the apex location of the travel-time hyperbola. These operator pair can be written as

$$\mathbf{d} = \mathbf{L}_h \mathbf{m}\,, \tag{6}$$
$$\tilde{\mathbf{m}} = \mathbf{L}_h^T \mathbf{d}\,. \tag{7}$$

However, not all signals in seismic data follow a hyperbolic (or apex shifted hyperbolic) travel times. For example, direct waves and surface waves can have a linear move-out pattern and the data can be modelled as follow

$$d(t,h) = \int_{v_{min}}^{v_{max}} m(\tau = t - hv, v)\, dv\,, \tag{8}$$

Again, expanding the modelling operator to allow for apex shifting, we get

$$d(t,h) = \int_{a_{min}}^{a_{max}} \int_{v_{min}}^{v_{max}} m(\tau = (t - (h-a)v, v)\, dv\, da\,, \tag{9}$$

and the adjoint will be

$$m(\tau,v,a) = \int_{h_{min}}^{h_{max}} d(t = (\tau + (h-a)v, h)\, dh\,. \tag{10}$$

Again, these operator pair can be rewritten as

$$\mathbf{d} = \mathbf{L}_\ell \mathbf{m}\,, \tag{11}$$
$$\tilde{\mathbf{m}} = \mathbf{L}_\ell^T \mathbf{d}\,. \tag{12}$$

Since seismic data can be assumed to be composed of both linear and hyperbolic events (Trad et al., 2001) , we can assume that the data can be modelled as follow

$$\mathbf{d} = \mathbf{L}_\ell \mathbf{m}_\ell + \mathbf{L}_h \mathbf{m}_h \,, \tag{13}$$

where $\mathbf{m}_\ell$ is the Radon model for the linear events and $\mathbf{m}_h$ is the Radon model for the hyperbolic events. The linear and hyperbolic modeling operators can be combined into one hybrid operator similar to the hybrid operators introduced by Nemeth et al. (2000) and Trad et al. (2001) to separate coherent noise. The hybrid Radon modelling operator can be represented by

$$\mathbf{d} = (\mathbf{L}_\ell \, \mathbf{L}_h) \begin{pmatrix} \mathbf{m}_\ell \\ \mathbf{m}_h \end{pmatrix} \,.$$

Then, the adjoint operator can be written as

$$\begin{pmatrix} \widetilde{\mathbf{m}}_\ell \\ \widetilde{\mathbf{m}}_h \end{pmatrix} = \begin{pmatrix} \mathbf{L}_\ell^T \\ \mathbf{L}_h^T \end{pmatrix} \mathbf{d} \,.$$

We can let the hybrid Radon operator be represented by

$$\mathbf{L} = \begin{pmatrix} \mathbf{L}_\ell \, \mathbf{L}_h \end{pmatrix} \,,$$

and the hybrid Radon model be represented by

$$\mathbf{m} = \begin{pmatrix} \mathbf{m}_\ell \\ \mathbf{m}_h \end{pmatrix} \,.$$

We can formulate an inversion-based deblending cost function to estimate the hybrid model as follow,

$$J = \|\mathbf{b} - \mathbf{\Gamma L m}\|_1^1 + \mu \|\mathbf{m}\|_1^1, \tag{14}$$

where $\mathbf{L}$ and $\mathbf{m}$ are the Radon hybrid operator, and Radon hybrid model of all common receiver gathers, $\mathbf{\Gamma}$ is the blending operator, and $\mathbf{b}$ is the blended data, and $\mathbf{D}$ is the separate shots data cube. The deblended shots can be estimated from the hybrid Radon model $\mathbf{m}$ by the forward modeling operator. The inversion cost function is minimized using Iteratively Re-weighted Least Squares (IRLS) algorithm. For more details regarding IRLS, please refer to Daubechies et al. (2010); Trad et al. (2003); Ibrahim and Sacchi (2014).

EXAMPLES

Synthetic Example

To test our deblending method using hybrid Radon transform, we use a numerically blended synthetic data set. The synthetic data were modeled using finite-difference modeling of the marmousi model using a Ricker wavelet of the central frequency of $15Hz$ as a source. The acquisition scenario represents two source boats firing near simultaneously. The source firing times are dithered using random time delays to make the source interferences appear incoherent, Figure 1 shows the sources firing times for both conventional and blended acquisitions. The results of the inversion based deblending are shown in Figure 2.

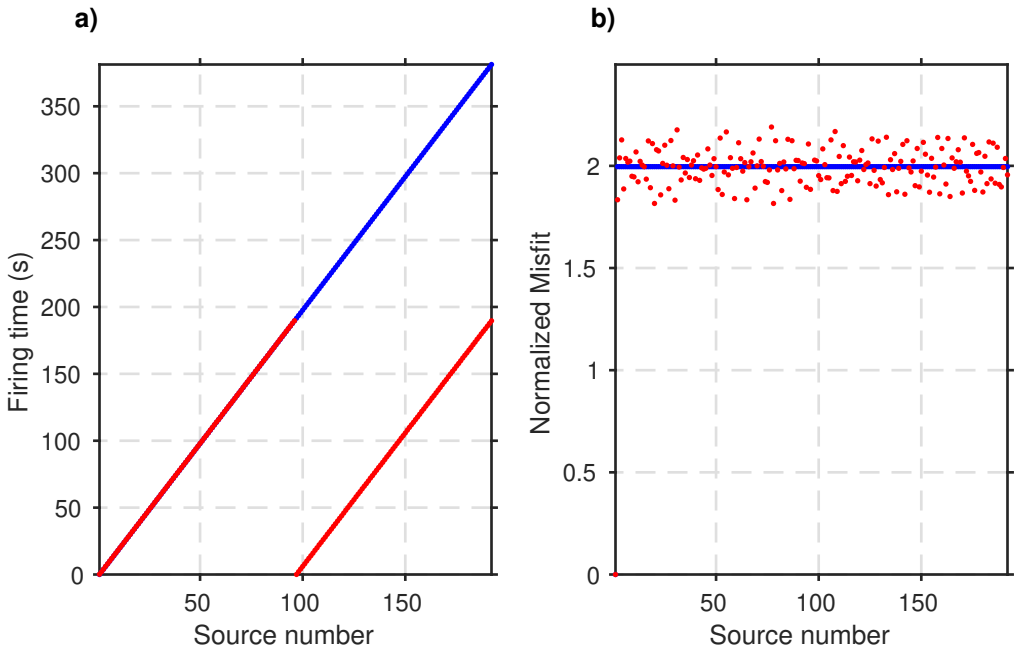

FIG. 1. Seismic sources firing times for Marmousi data example. (a) Firing times of conventional (blue) and simultaneous seismic sources (red). (b) Time delay between successive sources for conventional (blue) and simultaneous sources (red).

CONCLUSIONS

We implemented a hybrid Radon transform that combines apex shfited hyperbolic and linear basis functions in order to match seismic data more closely. The new hybrid transform is used in an inversion-based deblending algorithm. Results show that the new transform can be an efficient tool for accurately deblending seismic data that contain direct arrivals. Future work entails testing the hybrid transform for deblending land seismic data and separating surface waves.

ACKNOWLEDGMENTS

We thank the sponsors of CREWES for continued support. This work was funded by CREWES industrial sponsors and NSERC (Natural Science and Engineering Research Council of Canada) through the grant CRDPJ 461179-13.

REFERENCES

Berkhout, A. J., Blacquière, G., and Verschuur, E., 2008, From simultaneous shooting to blended acquisition: 78th Annual International Meeting, SEG, Expanded Abstracts, 2831–2838.

Berkhout, A. J., and Verschuur, D. J., 2006, Focal transformation, an imaging concept for signal restoration and noise removal: Geophysics, **71**, No. 6, A55–A59.

Chen, K., and Sacchi, M. D., 2015, Robust reduced-rank filtering for erratic seismic noise attenuation: Geophysics, **80**, No. 1, V1–V11.

Cheng, J., and Sacchi, M. D., 2015, Separation and reconstruction of simultaneous source data via iterative rank reduction: Geophysics, **80**, No. 4, V57–V66.

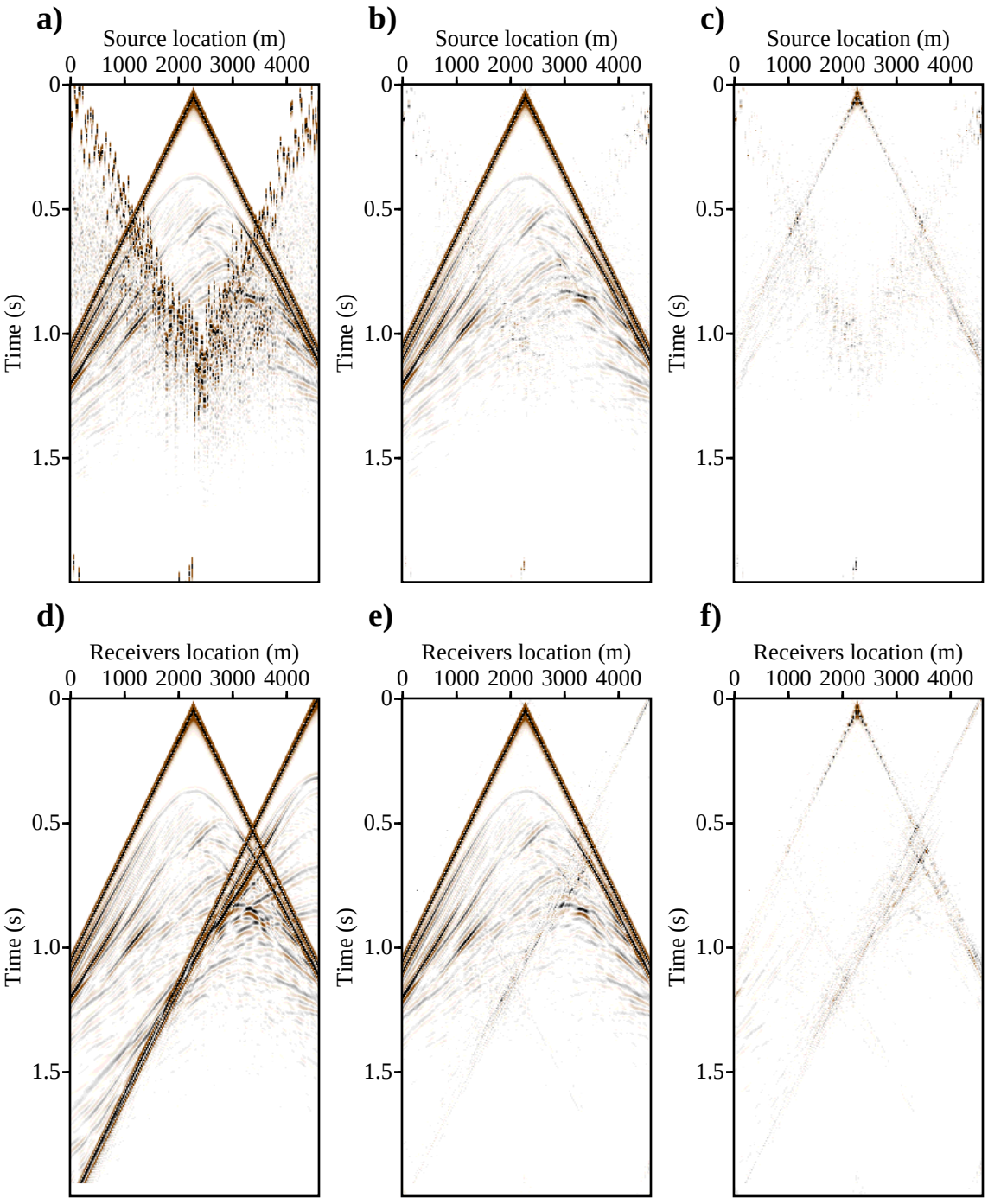

FIG. 2. Marmousi data example deblended using inversion approach. (a) Pseudo-deblended common receiver gather. (b) Inversion-based deblended common receiver gather. (c) Deblending error of common receiver gather. (d) Pseudo-deblended common source gather. (e) Inversion-based deblended common source gather. (f) Deblending error of common source gather.

Daubechies, I., DeVore, R., Fornasier, M., and Güntürk, C. S., 2010, Iteratively reweighted least squares minimization for sparse recovery: Communications on Pure and Applied Mathematics, **63**, No. 1, 1–38.

Fomel, S., and Liu, Y., 2010, Seislet transform and seislet frame: Geophysics, **75**, No. 3, V25–V38.

Herrmann, F. J., and Hennenfent, G., 2008, Non-parametric seismic data recovery with curvelet frames: Geophysical Journal International, **173**, No. 1, 233–248.

Ibrahim, A., 2015, Separating simultaneous seismic sources using robust inversion of Radon and migration operators: PhD Thesis, University of Alberta.

Ibrahim, A., and Sacchi, M. D., 2014, Simultaneous source separation using a robust Radon transform: Geophysics, **79**, No. 1, V1–V11.

Ibrahim, A., Terenghi, P., and Sacchi, M. D., 2018, Simultaneous reconstruction of seismic reflections and diffractions using a global hyperbolic radon dictionary: Geophysics, **83**, No. 6, V315–V323.

Nemeth, T., Sun, H., and Schuster, G. T., 2000, Separation of signal and coherent noise by migration filtering: Geophysics, **65**, No. 2, 574–583.

Sacchi, M., and Ulrych, T., 1995, Improving resolution of Radon operators using a model re-weighted least squares procedure: Journal of Seismic Exploration, **4**, 315–328.

Sacchi, M. D., Ulrych, T., and Walker, C., 1998, Interpolation and extrapolation using a high-resolution discrete Fourier transform: Signal Processing, IEEE Transactions on, **46**, No. 1, 31–38.

Shan, H., Ma, J., and Yang, H., 2009, Comparisons of wavelets, contourlets and curvelets in seismic denoising: Journal of Applied Geophysics, **69**, No. 2, 103 – 115.

Sinha, S., Routh, P. S., Anno, P. D., and Castagna, J. P., 2005, Spectral decomposition of seismic data with continuous-wavelet transform: Geophysics, **70**, No. 6, P19–P25.

Thorson, J. R., and Claerbout, J. F., 1985, Velocity-stack and slant-stack stochastic inversion: Geophysics, **50**, No. 12, 2727–2741.

Trad, D., Sacchi, M. D., and Ulrych, T. J., 2001, A hybrid linear-hyperbolic radon transform: Journal of Seismic Exploration, **9**, No. 4, 303–318.

Trad, D., Siliqi, R., Poole, G., and Boelle, J., 2012, Fast and robust deblending using apex shifted Radon transform: 82nd Annual International Meeting, SEG, Expanded Abstracts, **741**, 1–5.

Trad, D., Ulrych, T., and Sacchi, M., 2003, Latest views of the sparse Radon transform: Geophysics, **68**, No. 1, 386.

Yu, S., Ma, J., Zhang, X., and Sacchi, M. D., 2015, Interpolation and denoising of high-dimensional seismic data by learning a tight frame: Geophysics, **80**, No. 5, V119–V132.

Zhu, L., Liu, E., and McClellan, J. H., 2015, Seismic data denoising through multiscale and sparsity-promoting dictionary learning: Geophysics, **80**, No. 6, WD45–WD57.